Refining Spatial Proteomics by Mass Spectrometry: An Efficient Workflow Tailored for Archival Tissue

Author list

Rune Daucke[1], Charlotte V. Rift[2], Nicolai S. Bager[2], Kartikey Saxena[2], Peter R. Koffeldt[2], Jakob Woessmann[1], Valdemaras Petrosius[1], Eric Santoni-Rugiu[2], Bjarne W. kristensen[2], Pia Klausen[2] & Erwin M. Schoof[1]

Affiliations

[1] Department of Biotechnology and Biomedicine, Technical University of Denmark, 2800 Kgs. Lyngby, Denmark
[2] Department of Pathology, Copenhagen University Hospital Rigshospitalet, Blegdamsvej 9, DK-2100, Copenhagen Ø, Denmark.

Summary

Formalin-fixed paraffin-embedded (FFPE) tissue, while excellent for preserving tissue for extended periods of time, poses a challenge when extracting molecular information. We therefore developed an easily adaptable and highly efficient workflow for extracting high levels of proteins from low-input material. We compared sensitivity between two stains, EpCAM and H&E, across material inputs of 1,166 and ~800,000 μm^2. In the context of EpCAM-stained tissue, our investigations unveiled a range from ~1,200 unique protein groups at the lowest input to ~5,900 at the highest. For H&E, the spectrum covers ~900 to ~5,200 protein groups. We found an optimal balance between maximizing detected proteins and minimizing input material to be within the range of ~50,000 to ~100,000 μm^2. With this knowledge, we tested the spatial capabilities by isolating specific cell populations, through Laser Capture Microdissection (LCM), from three different tissue types, where we were able to identify tissue-specific signatures and prominent clustering of all cell populations.

Introduction

With its ease of handling and cost-efficient storage options, FFPE remains the prevailing method for preserving biological specimens for use in histopathology, resulting in the establishment of extensive repositories at pathology departments around the globe. These repositories hold enormous untapped potential for conducting retrospective studies (1,2). Yet, a prevailing limiting factor for the use of FFPE for proteomics has been the need for substantial sample quantities to acquire deep protein coverage, generally limiting FFPE proteomics by Mass Spectrometry (FFPE-MS) to bulk tissue analysis (3). This is highly problematic in the context of spatial proteomics, as it obscures the cell heterogeneity of the various cell populations within tissues such as cancer, which is defined by being exceptionally heterogeneous (4-8). In addition, there are limitations of available tissue associated with rare diseases, which can be too scarce or inadequately abundant to support comprehensive retrospective proteomic analyses.

The accelerated developments within the field of Liquid Chromatography-Mass Spectrometry (LC-MS) have recently enabled a level of sensitivity capable of analyzing ultra-low sample input (8,9), which consequently sparked a rapid emergence of methods transitioning from bulk or high-load input to low-load and near single-cell analysis (10-15). However, proteome coverage and ease of implementation on large-scale cohorts is still limited by sample preparation, which is especially true for FFPE tissue. We, therefore, developed an easily adaptable method for highly efficient protein extraction from LCM-collected FFPE samples. Samples were analyzed on a ThermoFisher Orbitrap Eclipse Tribrid Mass Spectrometer (MS) using our low-input tailored label-free acquisition WISH-DIA methods (16) combined with EvoSep One standardized high-throughput chromatography. Subsequently, raw data interpretation was performed in Spectronaut 18 without the use of spectral libraries to ensure biological and clinical significance. Our protocol builds on a similar approach introduced by Kwon et al., 2022 (10), where we collect the dissected tissue into an LC-MS compatible buffer, leaving no need for solid-phase extraction or other methods for sample clean-up. For any contaminants associated with the FFPE tissue itself, we rely on the C18 material within an EvoTip Pure to act as a filter, and disposable peptide trapping cartridge ensuring that material not compatible with LC-MS is not introduced to the analytical column.

We tested our workflow at different sample sizes to assess sensitivity and scalability. Likewise, we evaluated the efficiency of the staining methods EpCAM (Epithelial Cell Adhesion Molecule) and H&E (Hematoxylin and Eosin) to ensure the protocol is flexible across a diverse set of archival tissues. With the established workflow, we then

evaluated applicability to, and retrievability of biological relevance from the three types of cancer—glioblastoma (GB), Non-Small Cell Lung Cancer (NSCLC), and pancreatic ductal adenocarcinoma (PDAC). Here, we found distinct clustering between all cell types, along with prominent, cell-type-specific protein expressions, demonstrating a proof-of-principle that our workflow is applicable for exploring biological questions.

Materials and Methods

Tissue Preparation

Human pancreatic, lung, and brain surgical specimens were acquired with approval from the Ethics Committee prior to the initiation of the project (Pancreas: J. no: VD-2018-446, I-suite no. 6701 – Brain VEK: S-20150148 – Lung VEK: H-23021044). The tissue was fixed in 10% non-buffered formalin at a volume of around 10 - 20 times the volume of tissue for at least 24 hours. After fixation, a pathologist macrodissected the tissue, and tumor areas were selected for further analysis and embedded in paraffin. The FFPE tissue was dehydrated with an incremental increase from 70% ethanol to 100%. The dried tissue was cleared using Tissue-Clear®. Once cleared, the tissue was embedded in paraffin. PEN (Polyethylene naphtalate) membrane glass slides were UV-treated for 1 hour, followed by overnight drying at 37 °C in a Binder drying and heating chamber. The tissue was then sectioned into 5 µm thick slices using a rotation microtome and placed in a water bath at a temperature between 42 – 45 °C, depending on tissue composition, to “stretch” the paraffin and avoid folds and wrinkles. Following stretching, the tissue was then “scooped” up with the dried glass slide. The glass slide was left to dry at room temperature.

EpCAM Staining

The day before staining, slides were heated overnight at 56 °C in a Binder drying oven, followed by 60 °C for 1 hour before staining. Tissue sections were deparaffinized in Tissue-Clear® for 10 minutes and rehydrated with decreasing concentrations of ethanol. The membrane slides were then transferred to an automated immune stainer (Ventana Discovery). Antigen retrieval (pH 9.0) was performed at 95°C for 32 min. Blocking of endogenous peroxidase was achieved with Inhibitor CM (Roche). Afterward, sections were incubated with EpCAM (Ready-To-Use, 790-4465, Roche) for 60 minutes at room temperature, and the secondary antibody Omnimap Anti-Mouse (Roche) was applied. For detection, the antibody-antigen complex was visualized using Discovery Chromomap DAB-kit (Roche) according to the

manufacturer's instructions. The slides were counterstained with Hematoxylin II (Roche) for 8 minutes and Bluening Reagent for 4 minutes.

HE Staining

After adhesion, the slide was deparaffinized by submerging it in Tissue-Tek® Tissue-Clear® Xylene Substitute for 10 minutes, followed by 10 dips in 99% ethanol, another 10 dips in fresh 99% ethanol, 10 dips in 96% ethanol, and finally, 10 dips in 70% ethanol. After deparaffinization, the ethanol was removed by submerging the slide in a vessel with running demineralized water for 5 minutes. Following the washing, the slide was submerged in Mayer's hematoxylin for 4 minutes, running water for 5 minutes, 0.1% eosin in 0.1 M Walpole's acetate buffer for 1 minute, and finally, running water for 3 minutes. The slides were then left in the fume hood to dry overnight, after which they were stored in a closed container at room temperature.

Sample collection

Twenty microliters of 100 mM TEAB (triethylammonium bicarbonate) in MS-grade water were added to the lid of a 0.5 mL Protein LoBind® tube. We determined that 20 µL was the smallest volume capable of covering the entire surface of the lid, a critical factor when catapulting the tissue, as there is a high chance of losing samples if the tissue misses the buffer. The tubes were then individually loaded onto the ZEISS PALM Microbeam Laser Microdissection microscope using the SingleTube 500 CM II tube holder. Cell-dense areas between 1.166 µm² and 800,000 µm² with a thickness of 5 µm were collected in the buffer-filled lids, and collection was confirmed using a DinoLite digital microscope. Following the LCM collection, the tubes were spun down at 21,300 x G for 5 minutes to ensure that the tissue released from the lid of the tube.

Sample processing

The samples underwent boiling at 95 °C for 5 minutes, followed by sonication for 10 cycles of 30 seconds on, 30 seconds off using a Bioruptor® Pico sonicator. Water was pre-cooled to 4.0 °C and maintained at this temperature during sonication. After sonication, the samples were spun down at 21,300 x G for 30 seconds.

Digestion

To the samples, 10 µL of TEAB containing 1 ng of Pierce™ Trypsin/Lys-C Protease Mix MS-Grade per 25,000 µm² of tissue was added. The samples were left to digest overnight at 37°C with rotational shaking at 1,000 rpm. The following day, the samples were spun down at 21,300 x G for 30 seconds.

EvoTip Loading

To activate the C18 column in the EvoTips, 20 μL of 100% acetonitrile was added to each tip and spun through at 700 x G for 1 minute (all centrifugation steps were conducted at 700 x G). Subsequently, the tips were immersed in 100% isopropanol for 1 minute. Following this, 20 μL of MS-grade water with 0.1% formic acid (buffer A) was added and spun through. With the tips now activated, the sample was introduced and spun through. Afterward, the tips were spun through with 20 μL of buffer A. Finally, 250 μL of buffer A was added to the tips, followed by 10 seconds of centrifugation at 700 x G to ensure the liquid effectively submerged the C18-bound samples. Additionally, about 1/3 of the EvoTip box was filled with buffer A to prevent sample drying.

Liquid Chromatography settings

In our LC-MS/MS analysis, we employed the EvoSep One liquid chromatography system from Evosep Biosystems using the Whisper® 20 method. Peptides underwent separation over a 58-minute gradient (20 SPD), at a flow rate of 100 nL/min. The column utilized was a 15 cm × 75 µm with 1.7 µm C18 beads (Aurora Elite TS 15 cm nanoflow UHPLC column from IonOpticks). Mobile phases A and B comprised of LC-MS grade 0.1% formic acid in water and acetonitrile, respectively. The LC system was connected to an Orbitrap Eclipse Tribrid MS (ThermoFisher Scientific) through an EasySpray ion source linked to a FAIMSPro device.

Mass spectrometry settings

For mass spectrometry data acquisition, we employed our in-house developed WISH-DIA methods, which build on the HRMS1-DIA method by Xuan et al. (2020). The FAIMSPro device was operated in positive mode, with a compensation voltage of -45 V. MS1 scans were performed at a resolution of 120,000, with automatic gain control (AGC) set to 300%, and the maximum injection time set to auto. The mass-to-charge ratio (m/z) range was specified from 400 to 1000. Higher energy collisional dissociation

(HCD) was utilized for precursor fragmentation, with a normalized collision energy (NCE) of 33%, and the AGC target for MS2 was set to 1000%. Precursor ions were sequentially isolated in 17 m/z increments, scanned at a resolution of 120,000, with AGC set at 1000%, and the maximum injection set to auto.

Data analysis

The acquired raw MS data were analyzed using Spectronaut™ version 18 with the reviewed and filtered Homo sapiens library from UniProt, excluding isoforms (acquired on 14/08-2023). Spectronaut settings were maintained at factory configurations, except for specific modifications: "Enzymes / Cleavage Rules" were set to Trypsin and LysC, the fixed Carbamidomethyl (C) modification was removed, and "Quantity MS Level" was adjusted to MS1. Searches and quantification were carried out in batches according to experimental conditions for all samples (binned by tissue amount, sample type, etc.), and follow-up data analysis was performed in the R environment.

Results

Forming and optimizing a joined LCM and LC-MS/MS workflow

Our initial approach involved utilizing PALM LCM for tissue laser dissection and catapulting, employing commercially available LCM tubes with adhesive-filled caps. Unfortunately, this method posed challenges related to excessive tissue binding during protein extractions, which prompted a significant shift in our strategy. Initially inspired by Kwon et al. (2022) (10), we transitioned to a “hanging drop” method. This innovative approach involved capturing tissue into the lids of buffer-filled Protein LoBind tubes, successfully addressing the complications associated with tissue binding. The choice of buffers played a pivotal role in refining our proteomic workflow. After careful assessments, TEAB was identified as the most effective buffer, successfully addressing the challenges encountered in the initial phases (Figure 1A). The adoption of TEAB as an LC-MS compatible buffer marked a crucial advancement. This strategic modification eliminated the need for the labour-intensive SP3 clean-up process (18). Consequently, we observed an impressive nearly 100% increase in quantified protein IDs, achieving comparable depths with only half the tissue (Figure 1B). Importantly, this change did not compromise column longevity, indicating the successful mitigation of SP3-associated sample losses. Our optimization efforts extended to downstream processes, particularly focusing on the duration of tissue boiling and the impact of sonication (Figure 1C). Boiling FFPE tissue for five minutes proved to be an optimal

compromise, resulting in a 20% increase in detected proteins compared to scenarios with no boiling. Intriguingly, sonication did not significantly affect protein extraction but demonstrated a potential role in aiding tissue release, especially with cycles exceeding 10. With the refined workflow, we systematically evaluated its performance across different tissue amount, evaluating its ability to contruct quantitative proteome landscapes from cell-specific regions while maintaining information about their spatial localization. Additionally, we compared the EpCAM and H&E staining methods, revealing distinct drops in proteome coverage below 50,000 µm2, which is comparable to roughly 100 of the acinar pancreatic cells used. This specific range emerged as the optimal compromise, balancing the need for deep proteome coverage while conserving sample input requirements (Figure 1D). These results collectively demonstrate the adaptive nature of our tissue collection and lysis strategy, emphasizing the importance of methodological precision and strategic modifications in achieving robust spatial proteomic analyses.

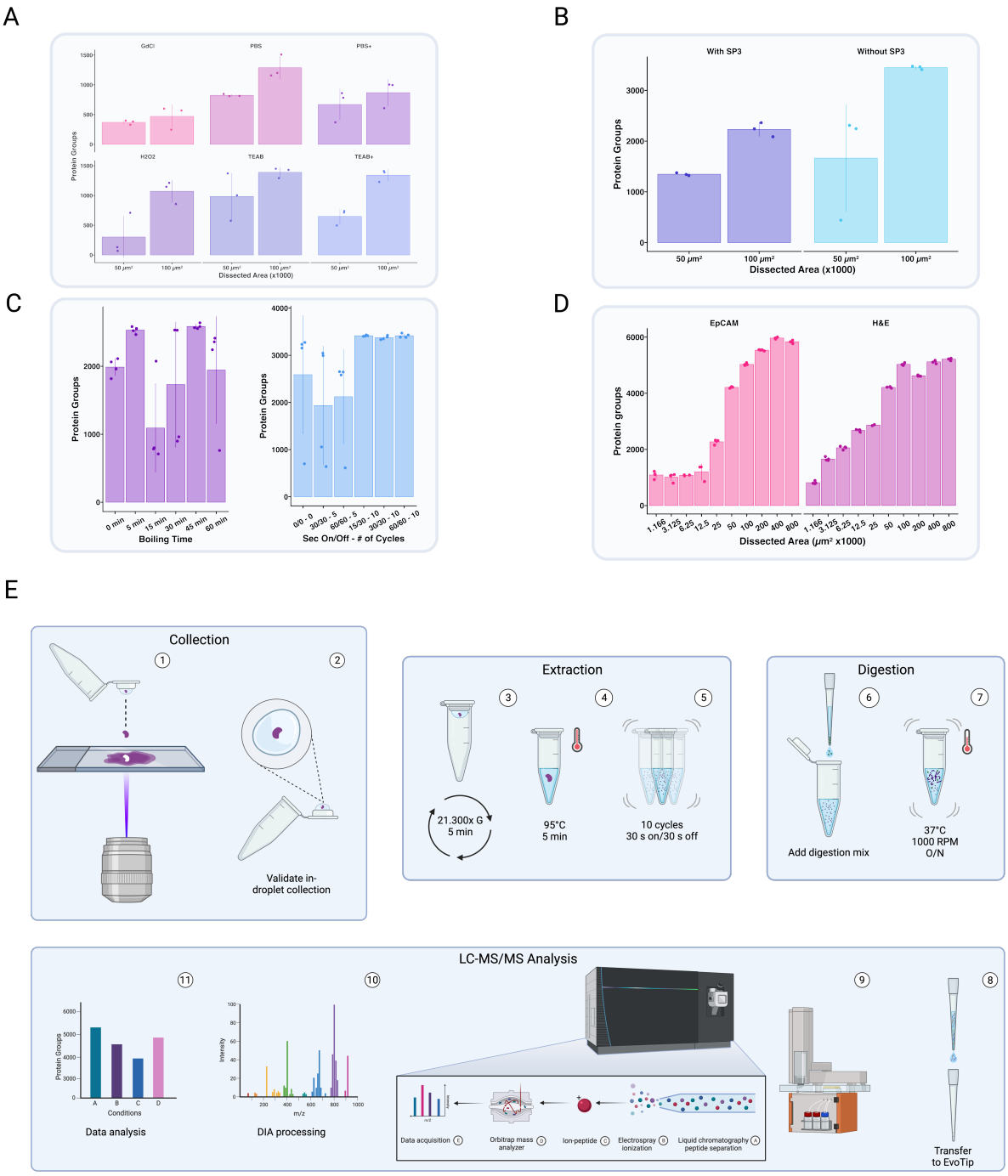

Figure 1. Workflow optimization overview on pancreatic acinar tissue. (A) Assessing different lysis buffers. TCEP and CAA is added to TEAB+ and PBS+. **(B)** Evaluating the impact of SP3 sample clean-up. **(C)** Downstream processing of collected tissue (50,000 µm²), with variations in boiling durations (on the left) and sonication periods and number of cycles (on the right). **(D)** Comparing our workflow on two common staining methods, EpCAM and H&E, across a wide arrange of tissue sizes. Samples with less than 50% proteome coverage is removed. **(E)** Full protocol, of our optimized workflow for LC-MS/MS analysis of LCM collected FFPE tissue.

Evaluating biological significance

To evaluate the applicability of our workflow across a wide range of tissue types, we next set out on a comprehensive evaluation across PDAC, GB, and NSCLC. Representative regions from each tissue type (50,000 μm^2) were isolated and subjected to our sample preparation and LC-MS acquisition. Distinct tissue clustering was observed in the heatmap and PCA plots, accompanied by prominent differential expression (Figure 2), showcasing a remarkable ability to discern proteomic landscapes and molecular complexities within the microenvironment of each cancer type. The adaptability of our optimized methodology was apparent across all types of tissue, revealing nuanced proteomic patterns and spatial distribution of proteins. Consistently, data suggests our optimized workflow to deliver spatial precision and in-depth analysis across diverse cancer types (Figure 2B). Positioned at the intersection of extensive proteome coverage and minimal sample input, it not only provides insights into each cancer type's unique molecular signatures but also promises to advance our understanding of the molecular intricacies inherent in different cancers. The systematic application of our refined methodology holds significant promise for furthering spatial biology research and enhancing our comprehension of complex molecular dynamics in various cancer types.

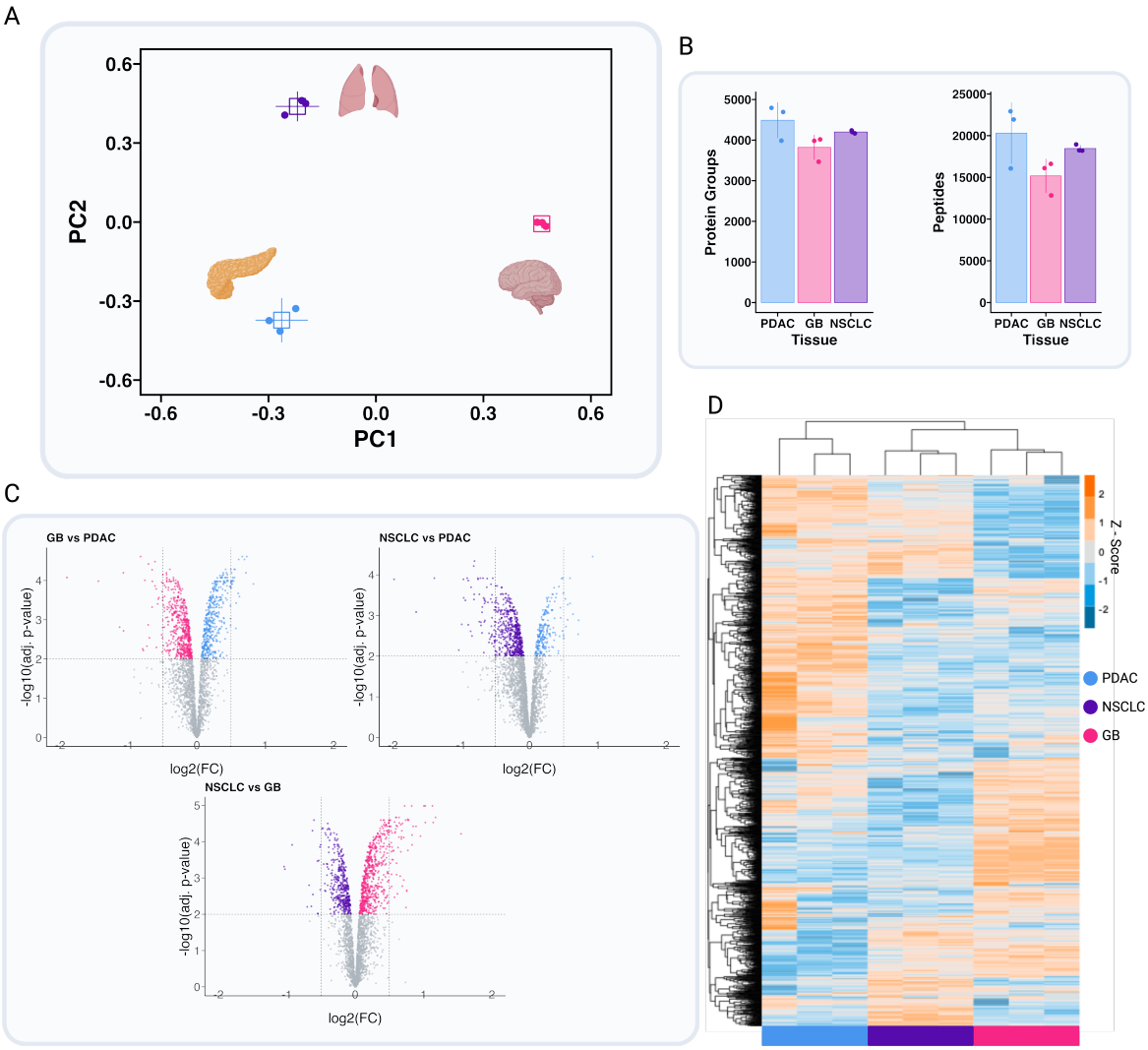

Figure 2. Assessing biological insight across various cancer types. (A) PCA plot showing distinct clustering of PDAC (blue), NSCLC (purple), and GB (pink). **(B)** Average number of protein groups (left) and peptides (right) detected from the three cancer types. **(C)** Volcano plots comparing differential expression between GB and PDAC (top left), NSCLC and PDAC (top right), and NSCLC and GB (bottom). **(D)** Heatmap showing relative up-regulated (orange) and down-regulated (blue) protein levels between the three cancer types.

Discussion

The challenges encountered with commercially available LCM tubes underscore the importance of tailoring methods to suit the unique requirements of LC-MS based spatial proteomics. The transition to a hanging drop method and adapted in a slightly altered fashion here, is a simple but effective adaptation to overcome the lack of commercially available, LC-MS focused consumables. This strategic adaptation not only resolved the initial adhesive issues but also contributed to the overall robustness of tissue capture. The elimination of SP3 clean-up in favor of an LC-MS compatible buffer allowed us to minimize sample loss, improve sample preparation reproducibility, and retain deep proteome coverage out of ultra-limited sample inputs. The substantial increase in quantified protein IDs, coupled with the absence of negative impacts on column longevity, highlights the efficiency gains achieved by this modification. However, shifting to in-droplet collection removed our ability to visually inspect collected tissue through a standard microscope. Therefore, we opted to inspect each collected sample through a DinoLite digital microscope to further ensure the robustness of our workflow, as samples that were ineffectively catapulted during LCM can be identified early in the workflow and discarded or recollected.

Refining downstream processes, particularly the duration of tissue boiling and the role of sonication, offers valuable insights. The optimal boiling time of five minutes, carefully balancing paraffin removal and throughput, underscores the significance of assessing each component of the protocol. This adjustment notably boosts throughput, cutting down general boiling times from 60 minutes to just 5 minutes, thus streamlining the entire workflow. While the impact of sonication on protein extraction is minimal, our results do hint at a potential role in easing tissue release, which, in turn, could increase workflow robustness. The systematic assessment across different tissue ratios and staining methods enriches our understanding of the versatility of our workflow. The identified compromise of 50,000 μm^2 for optimal proteome coverage is a crucial finding, balancing the depth of analysis with the imperative of conserving limited sample material. This insight positions the workflow as a valuable tool in the analysis of archival tissues. The systematic application of our refined methodology, positioned at the intersection of extensive proteome coverage and minimal sample input, not only offers insights into the unique molecular signatures of each presented cancer type, but also holds promise for advancing spatial biology research. Future applications may explore its potential in broader cancer research contexts, paving the way for a deeper understanding of the complex molecular dynamics inherent in various cancer types. Additional developments include the ability to downscale sample requirements even further, in a pursuit to enable spatial single-cell proteomics by MS

(scp-MS), similar to what is presented Makhmut et al. (2023) and Rosenberger et al. (2023).

In conclusion, our tailored spatial proteomics workflow for archival tissue emerges as a transformative approach, effectively overcoming challenges associated with FFPE samples and tissue heterogeneity. Designed for adaptability and efficiency, and relying on off-the-shelf consumables only, this method unlocks the potential of low-input materials for retrospective studies, tapping into extensive FFPE repositories. While efforts presented thus far have been primarily undertaken on the timsTOF platform from Bruker, we here attempted to evaluate the capability of Orbitrap-based instruments to pursue similar capabilities of low-input, spatial proteomics workflows. Across diverse cancer types, the workflow showcases its ability to unravel intricate proteome landscapes and molecular nuances within each microenvironment, and therefore appears primed to undertake data-driven investigations of cell-type specific proteome dynamics in primary clinical specimens.

References

1. Kokkat, T. J., Patel, M. S., McGarvey, D., LiVolsi, V. A., & Baloch, Z. W. (2013). Archived Formalin-Fixed Paraffin-Embedded (FFPE) Blocks: A Valuable Underexploited Resource for Extraction of DNA, RNA, and Protein. Biopreservation and Biobanking, 11(2), 101–106. https://doi.org/10.1089/bio.2012.0052
2. Eccher, A., Scarpa, A., & Dei Tos, A. P. (2023). Impact of a centralized archive for pathology laboratories on the health system. Pathology Research and Practice, 245, 154488. https://doi.org/10.1016/j.prp.2023.154488
3. Wiśniewski, J. R., Duś, K., & Mann, M. (2013). Proteomic workflow for analysis of archival formalin-fixed and paraffin-embedded clinical samples to a depth of 10000 proteins. Proteomics - Clinical Applications, 7(3-4), 225–233. https://doi.org/10.1002/prca.201200046
4. Ramón y Cajal, S., Sesé, M., Capdevila, C., Aasen, T., De Mattos-Arruda, L., Diaz-Cano, S. J., … Castellví, J. (2020). Clinical implications of intratumor heterogeneity: challenges and opportunities. Journal of Molecular Medicine, 98(2), 161–177. https://doi.org/10.1007/s00109-020-01874-2
5. Specht, H., & Slavov, N. (2018). Transformative Opportunities for Single-Cell Proteomics. Journal of Proteome Research, 17(8), 2565–2571. https://doi.org/10.1021/acs.jproteome.8b00257
6. Janku, F. (2014). Tumor heterogeneity in the clinic: Is it a real problem? Therapeutic Advances in Medical Oncology, 6(2), 43–51. https://doi.org/10.1177/1758834013517414
7. Zhu, L., Jiang, M., Wang, H., Sun, H., Zhu, J., Zhao, W., … He, Y. (2021). A narrative review of tumor heterogeneity and challenges to tumor drug therapy. Annals of Translational Medicine, 9(16), 1351. https://doi.org/10.21037/atm-21-1948
8. Valdemaras Petrosius, Pedro Aragon-Fernandez, Tabiwang N. Arrey, Nil Üresin, Benjamin Furtwängler, Hamish Stewart, Eduard Denisov, Johannes Petzoldt, Amelia C. Peterson, Christian Hock, Eugen Damoc, Alexander Makarov, Vlad Zabrouskov, Bo T. Porse, Erwin M. Schoof: Evaluating the capabilities of the Astral mass analyzer for single-cell proteomics. bioRxiv. Preprint. https://doi.org/10.1101/2023.06.06.543943
9. Brunner, A. D., Thielert, M., Vasilopoulou, C., Ammar, C., Coscia, F., Mund, A., … Mann, M. (2022). Ultra-high sensitivity mass spectrometry quantifies single-cell proteome changes upon perturbation. Molecular Systems Biology, 18(3), e10798. https://doi.org/10.15252/msb.202110798
10. Kwon, Y., Piehowski, P. D., Zhao, R., Sontag, R. L., Moore, R. J., Burnum-Johnson, K. E., … Zhu, Y. (2022). Hanging drop sample preparation improves sensitivity of spatial proteomics. Lab on a Chip, 22(15), 2869–2877. https://doi.org/10.1039/d2lc00384h
11. Mund, A., Coscia, F., Kriston, A., Hollandi, R., Kovács, F., Brunner, A. D., … Mann, M. (2022). Deep Visual Proteomics defines single-cell identity and heterogeneity. Nature Biotechnology, 40(8), 1231–1240. https://doi.org/10.1038/s41587-022-01302-5
12. Davis, S., Scott, C., Oetjen, J., Charles, P. D., Kessler, B. M., Ansorge, O., & Fischer, R. (2023). Deep topographic proteomics of a human brain tumour. Nature Communications, 14(1), 7710. https://doi.org/10.1038/s41467-023-43520-8

13. Makhmut, A., Qin, D., Fritzsche, S., Nimo, J., König, J., & Coscia, F. (2023). A framework for ultra-low-input spatial tissue proteomics. Cell Systems, 14(11), 1002–1014.e5. https://doi.org/10.1016/j.cels.2023.10.003
14. Anuar Makhmut, Di Qin, David Hartlmayr, Anjali Seth, Fabian Coscia: An automated and fast sample preparation workflow for laser microdissection guided ultrasensitive proteomics. bioRxiv. Preprint. https://doi.org/10.1101/2023.11.29.569257
15. Chen, H., Zhang, Y., Zhou, H., Chen, W., Peng, J., Feng, Y., … Liu, S. (2023). Routine Workflow of Spatial Proteomics on Micro-formalin-Fixed Paraffin-Embedded Tissues. Analytical Chemistry, 95(45), 16733–16743. https://doi.org/10.1021/acs.analchem.3c03848
16. Petrosius, V., Aragon-Fernandez, P., Üresin, N., Kovacs, G., Phlairaharn, T., Furtwängler, B., … Schoof, E. M. (2023). Exploration of cell state heterogeneity using single-cell proteomics through sensitivity-tailored data-independent acquisition. Nature Communications, 14(1), 5910. https://doi.org/10.1038/s41467-023-41602-1
17. Xuan, Y., Bateman, N. W., Gallien, S., Goetze, S., Zhou, Y., Navarro, P., … Conrads, T. P. (2020). Standardization and harmonization of distributed multi-center proteotype analysis supporting precision medicine studies. Nature Communications, 11(1), 5248. https://doi.org/10.1038/s41467-020-18904-9
18. Hughes, C. S., Moggridge, S., Müller, T., Sorensen, P. H., Morin, G. B., & Krijgsveld, J. (2019). Single-pot, solid-phase-enhanced sample preparation for proteomics experiments. Nature Protocols, 14(1), 68–85. https://doi.org/10.1038/s41596-018-0082-x
19. Rosenberger, F. A., Thielert, M., & Mann, M. (2023). Making single-cell proteomics biologically relevant. Nature Methods, 20(3), 320–323. https://doi.org/10.1038/s41592-023-01771-9

Acknowledgements

This work was funded by a grant from the Lundbeck foundation (R413-2022-869), the Independent Research Fund Denmark (2067-00053B), the Novo Nordisk Foundation (NNF21OC0071016), the Villum Foundation (00053026), and the Leo Foundation (LF-OC-21-000832) to E.M.S. The Novo Nordisk Foundation (NNF17OC0028636) was granted to Peter Vilmann and P.K. The Danish Cancer Society (R352-A20551) was granted to E.S.R. The Tømrermester Jørgen Holm og hustru Elisa f. Hansens Mindelegat was granted to Bojan Kovacevic and P.K. The Lundbeck foundation (R433-2023-218) was granted to B.W.K. The European Union's Horizon 2020 research and innovation programme under the Marie Sklodowska Curie grant agreement (101034291) was granted to Katrine Sonne Hansen on the behalf of the Biotech Research and Innovation Center. We also thank all members from the Cell Diversity Lab, headed by E.M.S. for constructive input and fruitful discussions, and the DTU Proteomics Core for technical instrument support.

Author contributions

E.M.S., P.K, and R.D. conceived and designed the project. R.D., P.K and E.M.S. performed experiments, N.S.B, K.S, and P.R.K aided in staining and sectioning of FFPE samples, and E.S.R, and B.W.K provided critical input. Data analysis was performed by R.D, J.W, and V.P. The manuscript was drafted and revised by R.D., E.M.S., C.V.R, and P.K with input from all other authors. E.M.S. and P.K supervised the work.

Competing interest

All other authors declare no competing interests.

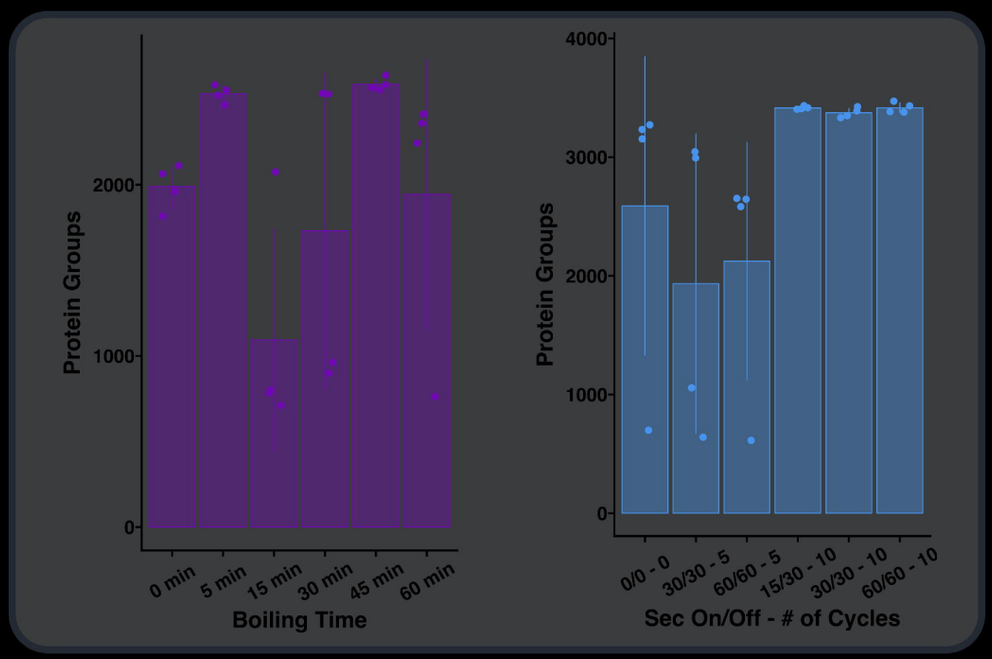
Protein Groups
0
1000
2000
0 min
5 min
15 min
30 min
45 min
60 min
Boiling Time
Protein Groups
0
1000
2000
3000
4000
0/0 - 0
30/30 - 5
60/60 - 5
15/30 - 10
30/30 - 10
60/60 - 10
Sec On/Off - # of Cycles

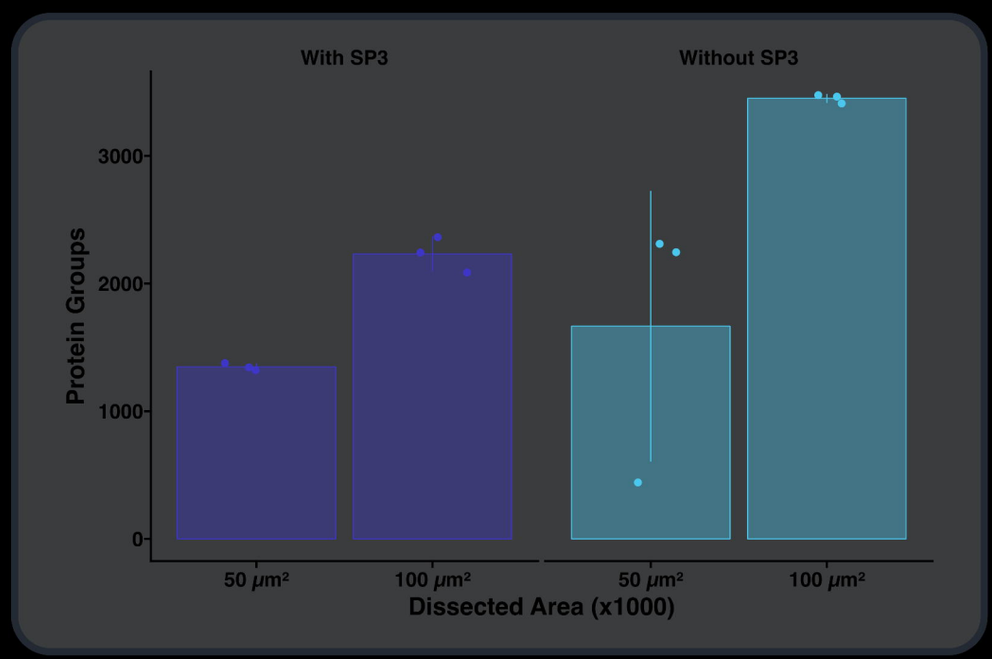
With SP3
Without SP3
Protein Groups
0
1000
2000
3000
50 µm²
100 µm²
50 µm²
100 µm²
Dissected Area (x1000)

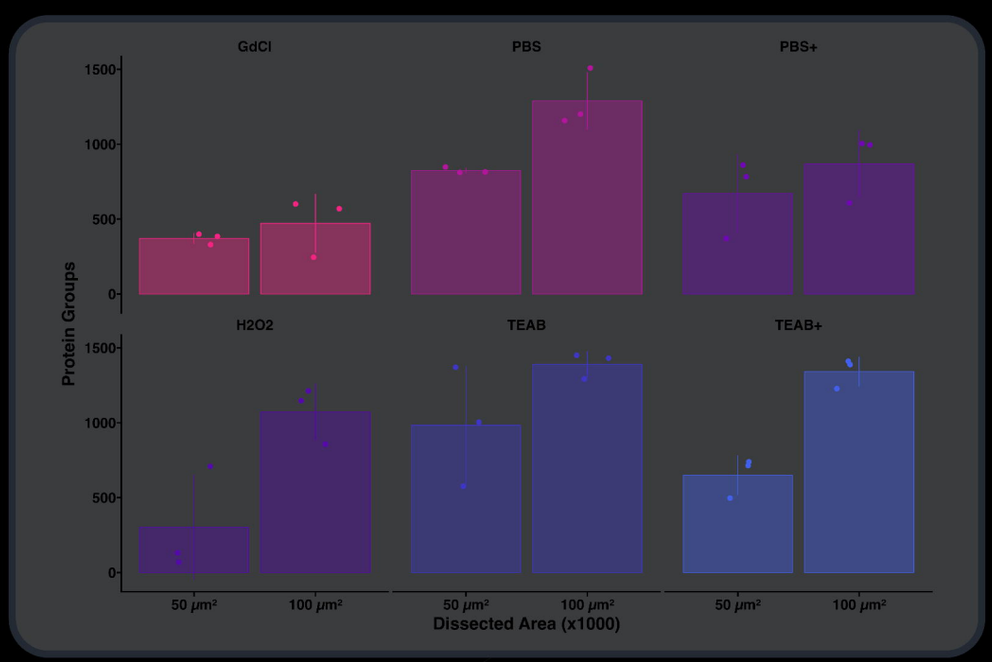
GdCl
PBS
PBS+
H2O2
TEAB
TEAB+
Protein Groups
0
500
1000
1500
50 µm²
100 µm²
50 µm²
100 µm²
50 µm²
100 µm²
Dissected Area (x1000)

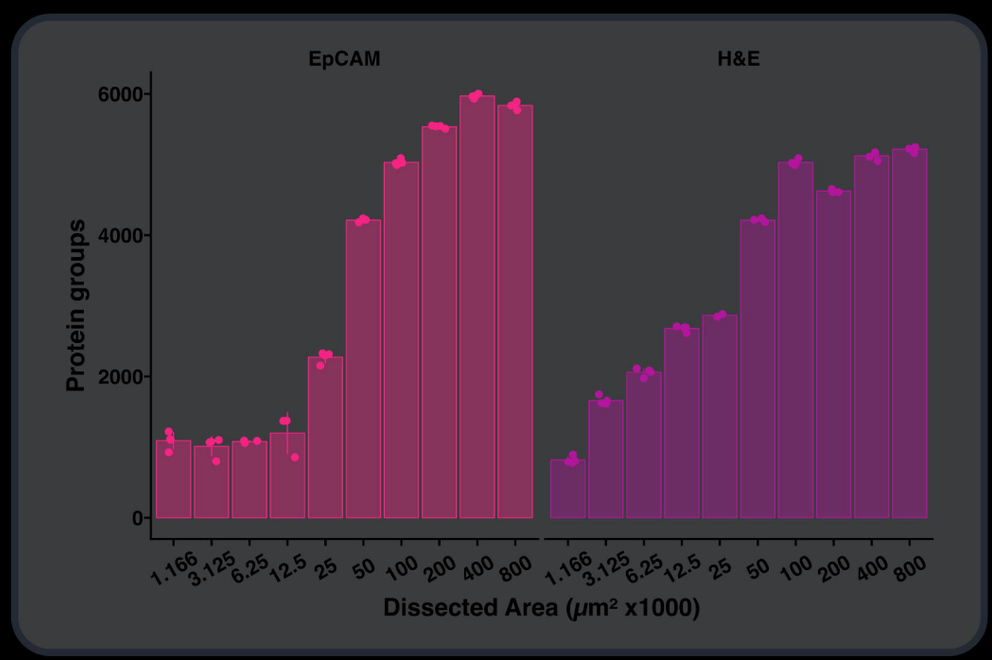
EpCAM
H&E
Protein groups
0
2000
4000
6000
1.166
3.125
6.25
12.5
25
50
100
200
400
800
Dissected Area (µm² x1000)

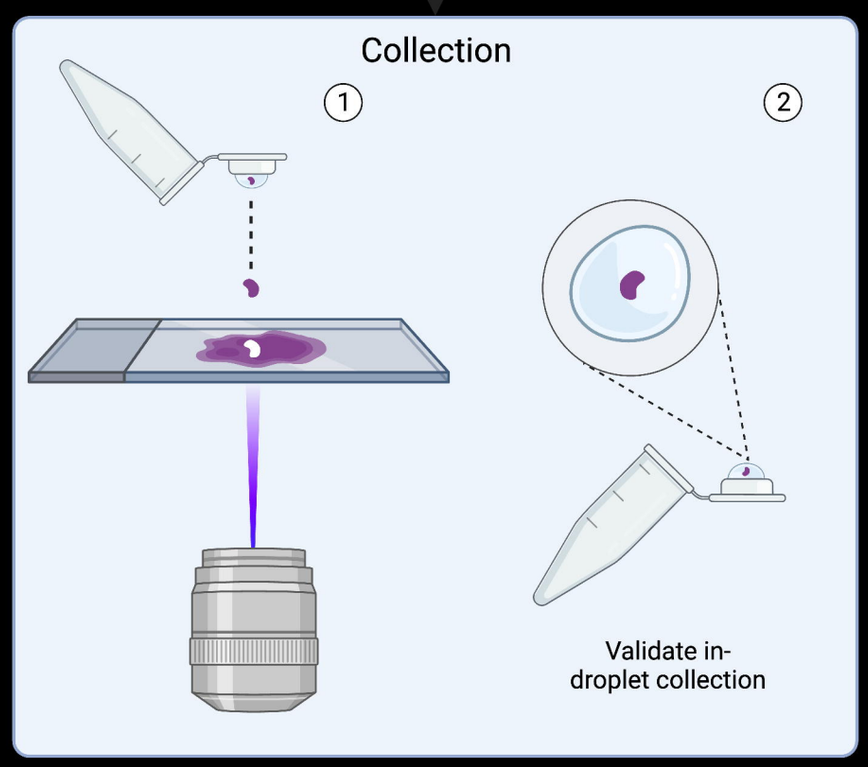
Collection
1
2
Validate in-
droplet collection

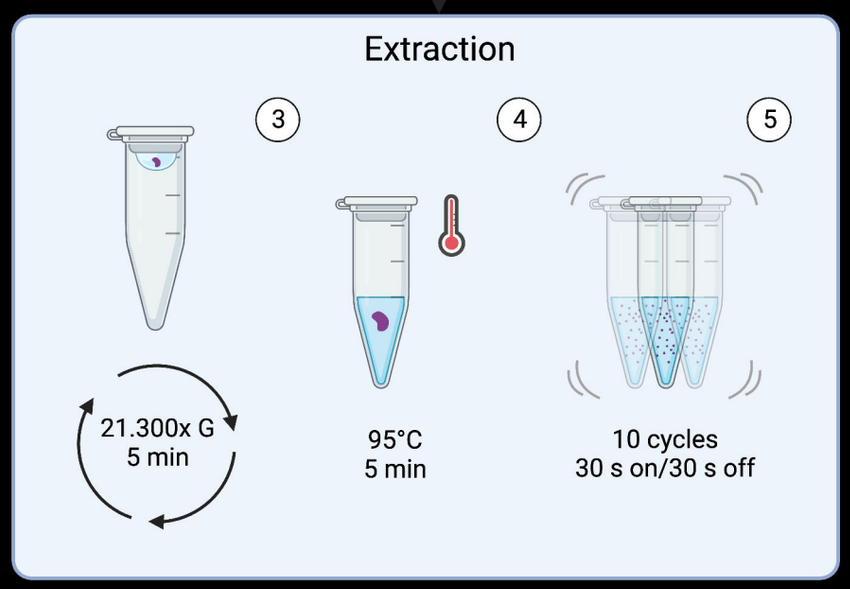
Extraction
3
4
5
21.300x G
5 min
95°C
5 min
10 cycles
30 s on/30 s off

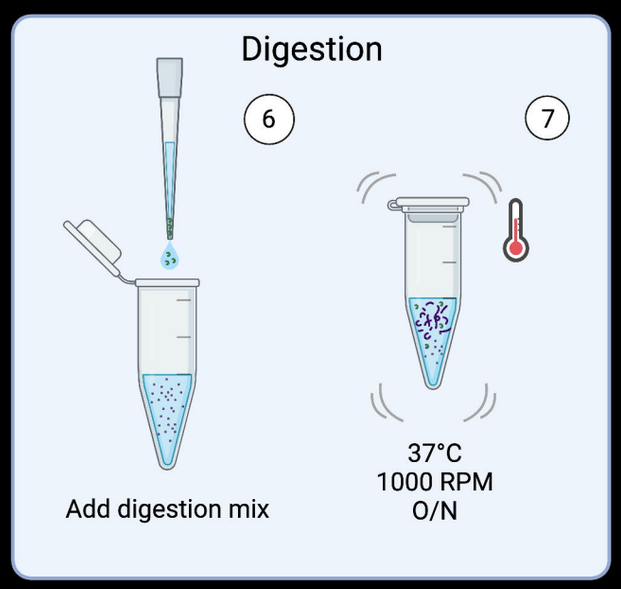
Digestion
6
7
Add digestion mix
37°C
1000 RPM
O/N

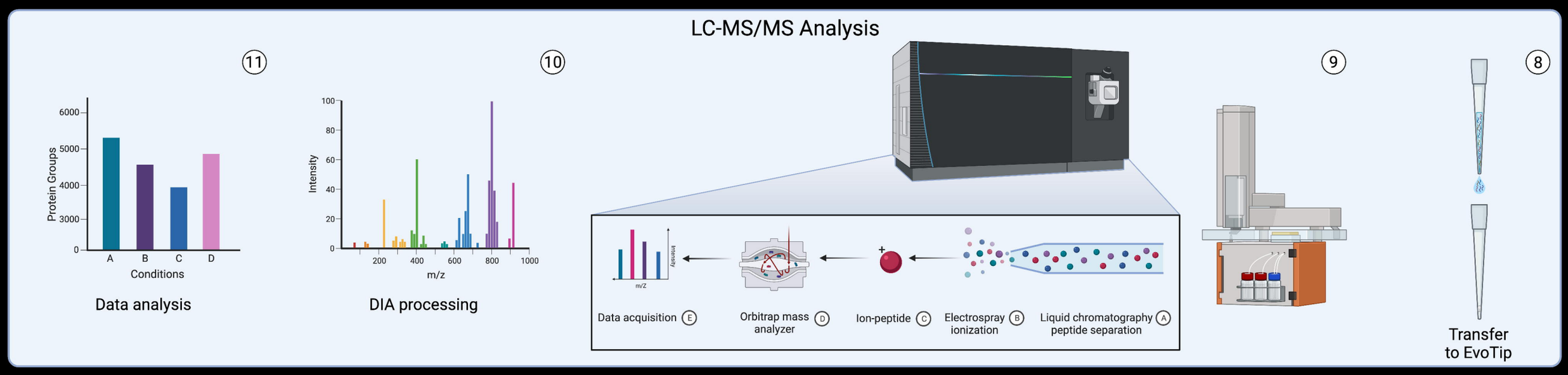
LC-MS/MS Analysis
11
10
9
8
Protein Groups
0
3000
4000
5000
6000
A
B
C
D
Conditions
Data analysis
Intensity
0
20
40
60
80
100
200
400
600
800
1000
m/z
DIA processing
Data acquisition E
Orbitrap mass analyzer D
Ion-peptide C
Electrospray ionization B
Liquid chromatography peptide separation A
Transfer
to EvoTip

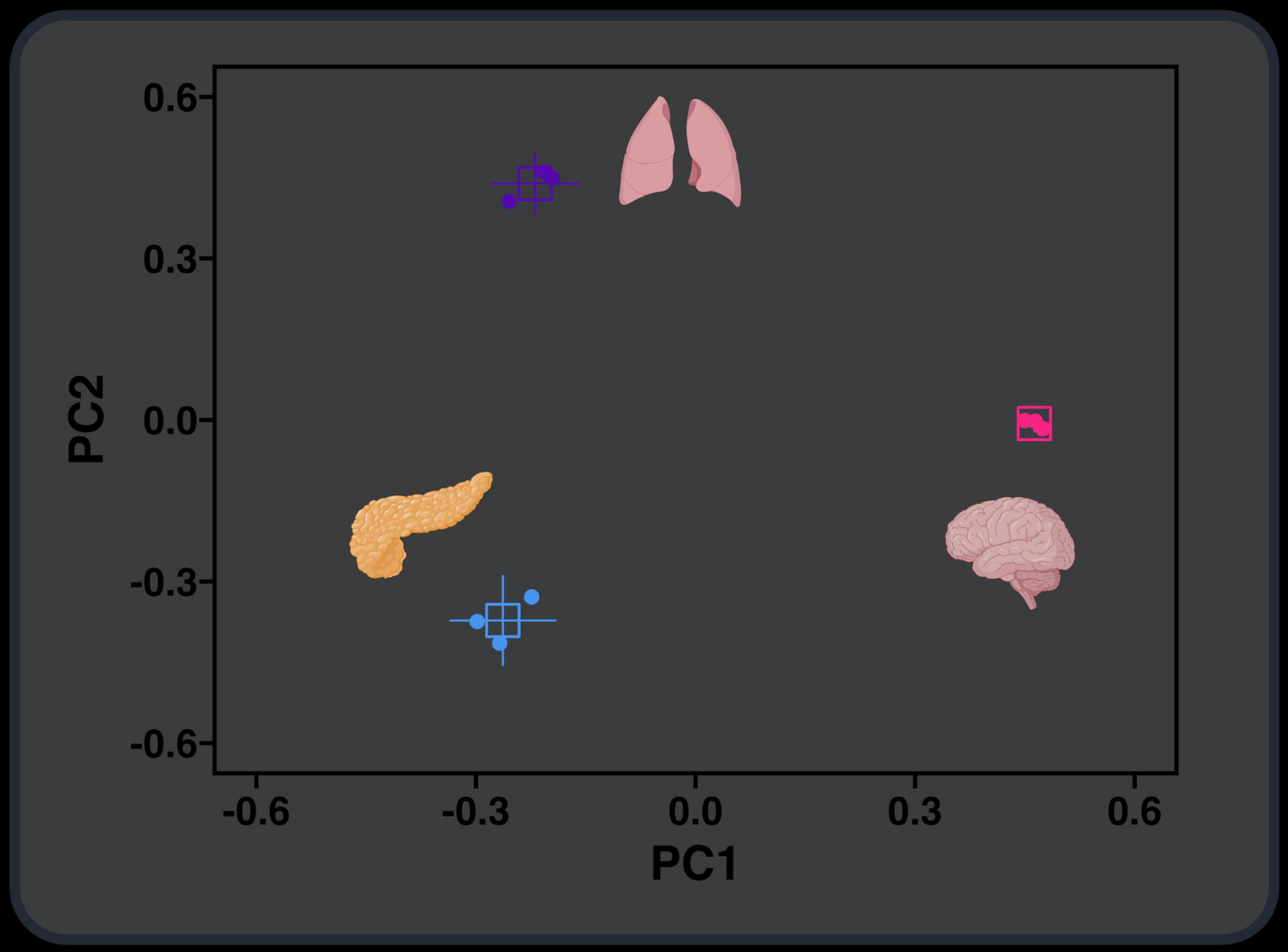
PC2
PC1
0.6
0.3
0.0
-0.3
-0.6

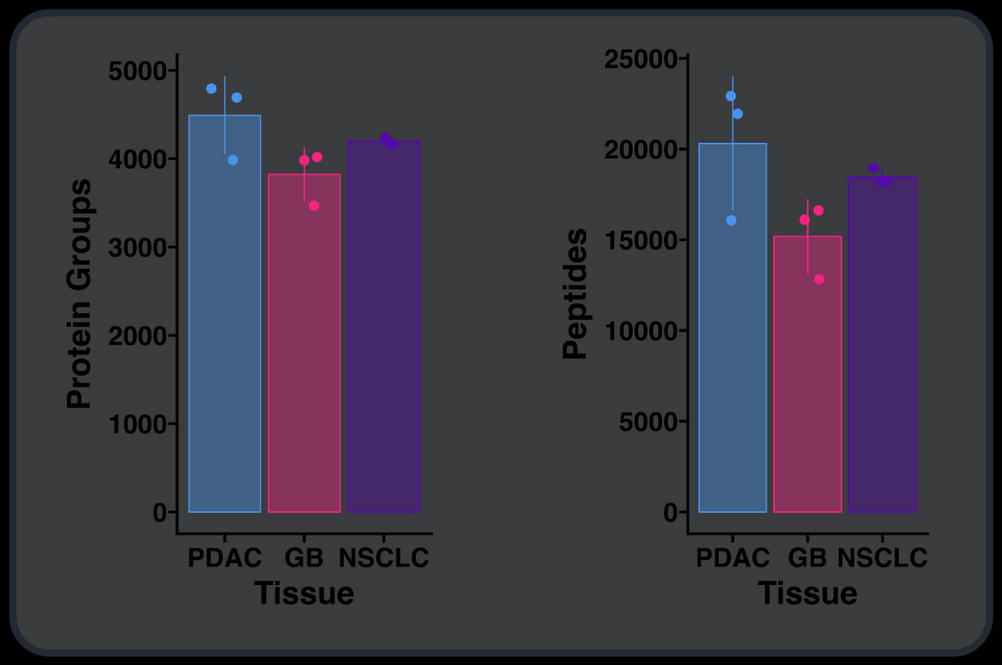
Protein Groups
Peptides
Tissue
PDAC
GB
NSCLC

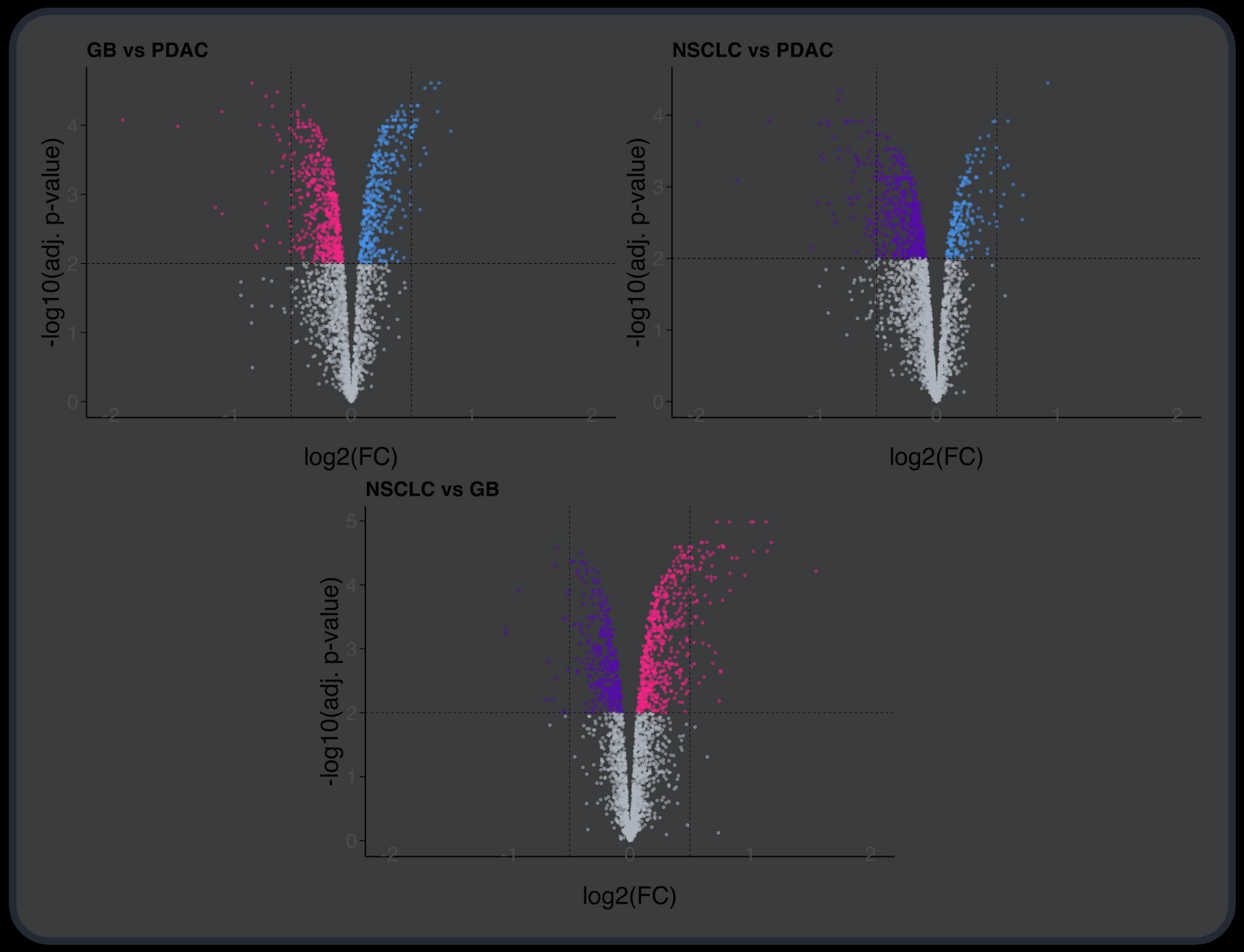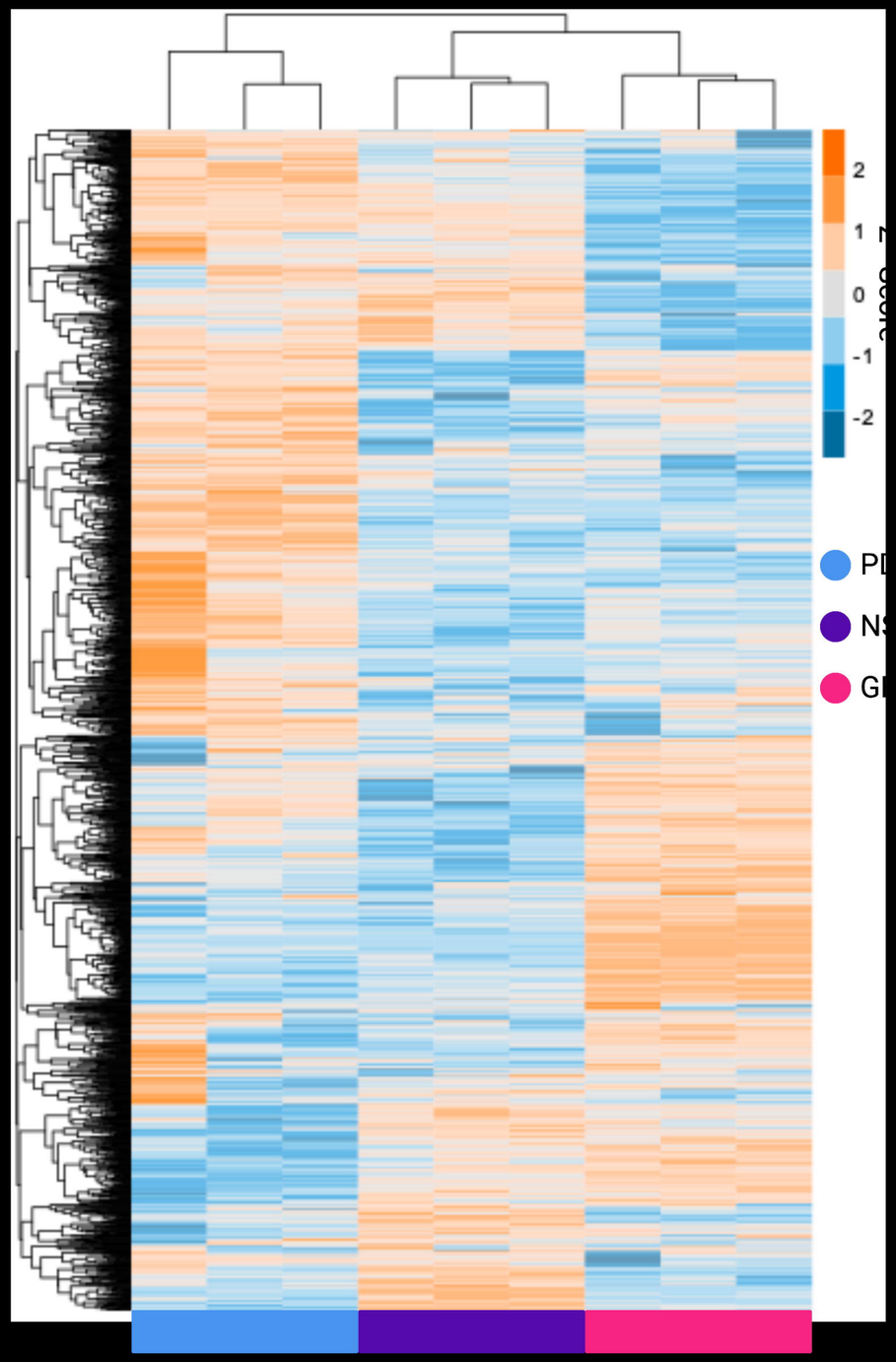
GB vs PDAC
NSCLC vs PDAC
NSCLC vs GB
-log10(adj. p-value)
log2(FC)